Nonreciprocal Reflection-Beam Isolators for Far-Infrared Use

MOTOHISA KANDA AND WILLIAM G. MAY, MEMBER, IEEE

***Abstract*—Magnetoplasma reflection-beam isolators for submillimeter-wave use are discussed in theory and experiment. The basic device uses the Kerr transverse magnetooptic effect (plane of polarization of the EM wave in the plane of incidence, which is perpendicular to a dc magnetic field) in InSb near room temperature. When the semiconductor slab is covered with a thin dielectric layer acting as a matching transformer, improved performance is predicted and observed at 337 μm, and very efficient isolator performance is predicted for 118 μm. Physical arguments are presented to explain the nonreciprocal phenomenon and lead to better device design.**

I. Introduction

THE PURPOSE of this paper is to discuss magnetoplasma reflection-beam isolators for far-IR use. The basic geometry chosen has the plane of polarization of the EM waves in the plane of incidence, and the direction of propagation is perpendicular to a dc magnetic field which is parallel to the surface of the magnetoplasma (Kerr transverse magnetooptical effect). This paper will present some refinements of the basic geometry leading to good isolator design. Both theoretical and experimental behavior of a new, practical geometry will be given.

II. General Discussion

Various studies of the basic geometry have been made. Barber and Crombie [1] have calculated the reflection coefficient from a sharply bounded ionosphere and found that the reflection for waves propagating from west to east was greater than for east to west propagation. Nonreciprocal reflection of EM waves incident on a solid-state magnetoplasma has been studied at 94 GHz [2], [3] and at 337 μm [3], [4]. For the basic geometry, no choice of parameters was found which gave a very large ratio of forward-to-reverse reflection coefficient along with low forward loss, as would be required for an efficient isolator. Some details of these calculations will be summarized below, along with the discussion of better geometries.

One significant difference between the ionospheric case and a solid-state magnetoplasma is the presence in the latter of the large, background permittivity ($K_L = 12$ to 18 for many semiconductors) which caused the reverse reflection coefficient to be rather large. With this in mind, two similar structures using the same basic relation of incident electric field, surface plane, and magnetic field are also considered: 1) free space replaced by a medium of high dielectric constant [3]; and 2) the plasma covered with a relatively thin dielectric layer. This latter geometry seemed promising in fabrication and performance and is the one analyzed in most detail below. Theoretical results for the various structures will be compared, as well as some experimental results at 337 μm for the best geometry. We also give a physical explanation of the nonreciprocal reflection coefficient more thorough than has been presented before.

III. Calculation of Reflection Coefficient

In this section we derive the reflection coefficient R_0 for the interface between free space and a dielectric coated magnetoplasma as shown in Fig. 1, using a transmission-line impedance method. The reflection coefficient for the other configurations mentioned above may be found by simplifying the results of this section. Some of these results may be found in [3].

For convenience we characterize the solid-state plasma as a medium with a complex dielectric tensor. In the calculations we assume the simplest case, where the carrier effective mass m^* is isotropic, as is the collision time τ which is also independent of energy. Quantum effects are ignored. We choose a coordinate system such that B_0 is parallel to the positive z axis. Then the dielectric tensor $\overline{\overline{K}}$ in the case of a single type of carrier and intraband effects becomes

$$\overline{\overline{K}} = \begin{vmatrix} K_\perp & -K_x & 0 \\ K_x & K_\perp & 0 \\ 0 & 0 & K_\parallel \end{vmatrix} \tag{1}$$

where

$$K_\perp = K_L - \frac{j\omega_p^2}{\omega}\left[\frac{(j\omega\tau+1)\tau}{(j\omega\tau+1)^2+(\omega_c\tau)^2}\right] \tag{2}$$

$$K_x = -\frac{j\omega_p^2}{\omega}\left[\frac{\omega_c\tau^2}{(j\omega\tau+1)^2+(\omega_c\tau)^2}\right] \tag{3}$$

$$K_\parallel = K_L - \frac{j\omega_p^2}{\omega}\left[\frac{\tau}{j\omega\tau+1}\right] \tag{4}$$

and

$$\omega_p^2 = ne^2/m^*\epsilon_0 \tag{5}$$

$$\omega_c = eB_0/m^*. \tag{6}$$

The wave impedance G for the wave transmitted past an interface is defined by

$$G^t = -\frac{E_x^t}{H_z^t} \tag{7}$$

and for the reflected wave,

$$G^r = \frac{E_x^r}{H_z^r} \tag{8}$$

where superscripts t and r specify components traveling in the direction of the transmitted and reflected waves, respectively. The wave impedance G for each layer shown in Fig. 1 is as

Manuscript received May 14, 1973; revised July 24, 1973. This work was supported by NASA, under Grant NGL 06-003-088.

M. Kanda was with the Department of Electrical Engineering, University of Colorado, Boulder, Colo. 80302. He is now with the Noise and Interference Section, Electromagnetics Division, National Bureau of Standards, Boulder, Colo. 80302.

W. G. May is with the Department of Electrical Engineering, University of Colorado, Boulder, Colo. 80302.

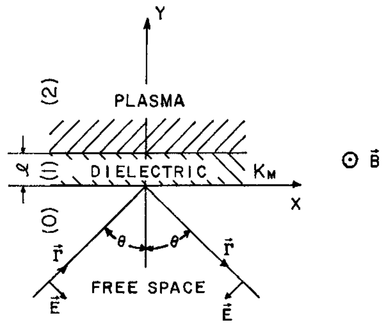

Fig. 1. Orientations of field vector E, propagation vector Γ, and dc magnetic field B.

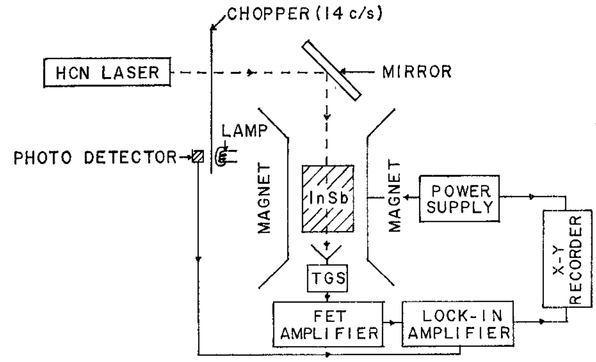

Fig. 2. Block diagram for IR experimental setup.

follows. In free space (region 0):

$$G_0^t = G_0^r = Z_0 \cos\theta. \tag{9}$$

In the dielectric medium (region 1):

$$G_1^t = G_1^r = \frac{Z_0}{K_M}(K_M - \sin^2\theta)^{1/2} \tag{10}$$

where K_M is the relative dielectric constant of the medium. In the magnetoplasma (region 2):

$$G_2^t = Z_0\left[A\cdot\left(\frac{1}{A} - \sin^2\theta\right)^{1/2} + D\cdot\sin\theta\right] \tag{11}$$

$$G_2^r = Z_0\left[A\cdot\left(\frac{1}{A} - \sin^2\theta\right)^{1/2} - D\cdot\sin\theta\right]. \tag{12}$$

Here A and D are:

$$A = \frac{K_\perp}{K_\perp^2 + K_x^2} \tag{13}$$

$$D = -\frac{K_x}{K_\perp^2 + K_x^2}. \tag{14}$$

Unlike the case for an isotropic medium where K_x is zero, here G_2^t and G_2^r are unequal.

The reflection coefficients for H and for E at the interface $y=l$ in Fig. 1 are given by

$$R_1 = \frac{H_z^r}{H_z^t} = \frac{G_1^t - G_2^t}{G_1^r + G_2^t} \tag{15}$$

and

$$r_1 = \frac{E_x^r}{E_x^t} = \frac{\dfrac{1}{G_1^t} - \dfrac{1}{G_2^t}}{\dfrac{1}{G_1^r} + \dfrac{1}{G_2^t}} \tag{16}$$

with field quantities evaluated in region 1. From analogy with transmission-line theory, the overall effective impedance Z_1 seen for the structure at the interface $y=0$ is given by

$$Z_1 = G_1^t\left[\frac{1 + r_1\exp(-j2k_1l)}{1 + R_1\exp(-j2k_1l)}\right] \tag{17}$$

where $k_1 = k_0(K_M - \sin^2\theta)^{1/2}$ is the wavenumber in the dielectric medium, and l is the thickness of the dielectric layer.

Finally, the complete reflection coefficient for a wave reflected from the structure of Fig. 1 is given by

$$R_0 = \frac{G_0^t - Z_1}{G_0^r + Z_1}. \tag{18}$$

If the plasma is lossless, there will be a change of phase but no change in magnitude of R_0 upon reversal of direction. However, if D given in (14) is complex, due to the presence of loss in the magnetoplasma, the reflection coefficient R_0 is found to be nonreciprocal; that is, reversal of the direction of propagation, or alternatively the sense of the dc magnetic field, changes the magnitude of the reflection coefficient.

IV. Experimental Procedure

Experiments were performed at 337 μm using n-type InSb as the plasma. This material had electron mobility $\mu = 7.4 \times 10^4$ cm^2/V·s, $n = 1.25 \times 10^{16}$ electrons/cm^3 near room temperature, and we assumed that $K_L = 17.9$ and $m^* = 0.021\ m_0$.

The InSb was mechanically polished and chemically etched. The dielectric layer was of high-density polyethylene with $K_M = 2.27$ and a thickness l typically 0.2 mm, as shown in Fig. 1. The block diagram of the experimental apparatus used to measure the nonreciprocal reflection is shown in Fig. 2. The sample was placed in the 1-in airgap of a 6-in Varian magnet which provided a maximum magnetic field of 15 kG.

An HCN laser operating at 337 μm provided a stable linearly polarized output of approximately 10 mW CW which was extracted from a beam splitter and passed through a lens used as a window to focus the beam onto the sample; the beam angle was approximately 3°. The reflected wave from the sample was received by a pyroelectric detector mounted in a horn. Reflection and insertion loss values from the structure were measured with respect to polished brass.

V. Theoretical and Experimental Results

This section compares the theoretical and experimental results for the various geometries. Reflection losses from the interface between free space and InSb at 284 K were measured as a function of incident angle and dc magnetic field. There was general agreement between theoretical and experimental results, but the maximum isolation was only about 3 dB with 2 dB of forward loss. Since the high-lattice dielectric constant in InSb ($K_L = 17.9$) destroys large nonreciprocal reflection, the reflection from the interface between a semiinfinite medium with dielectric constant K_M and a solid-state plasma was considered as has been previously reported [3] just as for

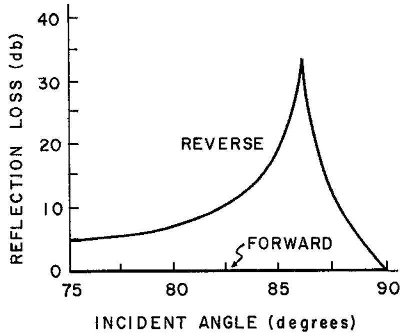

Fig. 3. Theoretical reflection loss of InSb at 337 μm as a function of incident angles. The InSb is assumed in a magnetic field of 13.2 kG and in a medium with $K_M = 30$.

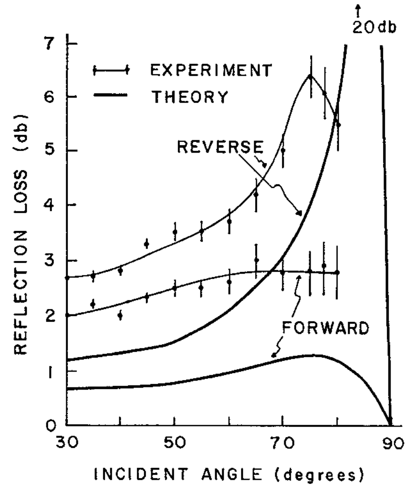

Fig. 4. Theoretical and experimental reflection loss of InSb at 337 μm as a function of incident angle. Geometry of the isolator is shown in Fig. 1, with $l = 250$ μm and $B = 15$ kG.

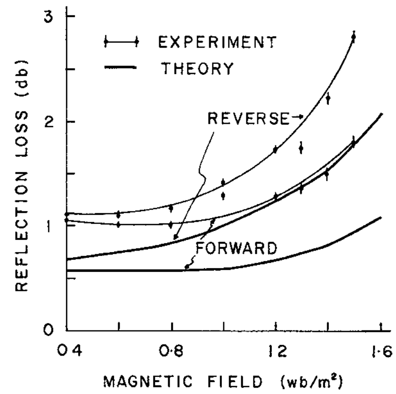

Fig. 5. Theoretical and experimental reflection loss for InSb at 337 μm as a function of magnetic field. Geometry of the isolator is shown in Fig. 1, with $l = 250$ μm and $\theta = 65°$.

the 94-GHz reflection-beam isolator. The theoretical reflection loss from the interface between dielectric with $K_M = 30$ and intrinsic InSb at a wavelength of 337 μm and at 300 K and dc magnetic field of 13.2 kG was calculated [3]–[5] and is shown again here in Fig. 3 for comparison to the more practical results below. Isolation of 34 dB with 0.5-dB insertion loss is predicted at an incident angle of 85.5°. The theory predicts much poorer isolation for smaller K_M, i.e., $K_M < 20$. The necessity of the dielectric medium whose dielectric constant is 30, however, makes this experiment difficult. The various materials such as rutile and barium titanate which are known to have high dielectric constants are quite lossy at 337-μm wavelength. The few materials known to be transparent at this wavelength, such as some semiconductors, polyethylene, Teflon, and quartz, typically have a dielectric constant of around 10 or less, and none of these is even close to what is required ($K_M = 30$).

In order to overcome this difficulty, we introduce a new geometry consisting of a thin dielectric layer placed on top of the InSb as a matching transformer. The idea of this configuration is to create the same effect as a reflection from the interface between the high-permittivity medium ($K_M = 30$) and InSb by adjusting the thickness of a dielectric layer of small permittivity. The dielectric material chosen for this layer was high-density polyethylene whose dielectric constant is 2.27, and loss tangent as low as 1.3×10^{-3} at 337 μm [6].

The theoretical and experimental reflection losses from the interface between free space and dielectric coated intrinsic InSb at 284 K are shown in Fig. 4 for the dc magnetic field of 15 kG as a function of incident angle, and in Fig. 5 at fixed angle of 65° as a function of dc magnetic field. The thickness of the polyethylene layer was 250 μm.

The experiments verify the theory for incident angles less than 80°, and general agreement between theoretical and experimental results is acceptable within experimental errors. Experimental difficulties caused poor results for larger incident angles. The output power from HCN laser has an angular spread of around 1° onto the sample depending on the tilt of the sample to the laser window. Therefore, the reflection obtained from the experiments was an "average" value of reflection for an angular spread. The spread in incident angles not only smeared out the sharpness, but also reduced the peak of the reflection curve. Therefore, the error caused by this source was significant, especially at large incident angles where the reflection coefficient changes rapidly with incident angle (see Fig. 4). Effort was thus made to shift the isolation peak to a smaller angle, as discussed below.

VI. Discussion and Conclusions

In this section we discuss the physical origins of the nonreciprocity of the structure. Quantities such as the ellipticity of the electric field and the orbit of electrons in the plasma are evaluated to gain a physical understanding of the nonreciprocal phenomena. Finally, applications of the device and possible further refinements for isolators are also discussed.

A. Physical Explanation of Nonreciprocity

A dc magnetic field makes the plasma anisotropic because a transverse velocity of the electrons interacts with the field to produce motion in the Hall or $\boldsymbol{v} \times \boldsymbol{B}$ direction. As a result, the conductivity and dielectric constants become tensors. It can be shown that the nature of the magnetic force is such that the off-diagonal terms are linear in the dc magnetic field as long as the field is small. This anisotropic effect in the plasma is an essential factor for nonreciprocity.

In the case of propagation transverse to a dc magnetic field, the propagation constant in infinite magnetoplasmas can easily be shown to be reciprocal. Thus the question arises why nonreciprocal reflection can take place at all. To answer this let us consider the excitation of EM waves from an incident plane wave on a semiinfinite magnetoplasma.

The nonreciprocity arises from the interface between free space and the plasma. Coupling between the x and y components of the electric field through the dc magnetic field is expected from the Hall current due to the tensor nature of the permittivity. Since the Hall current has a definite sense with respect to the dc magnetic field, the amplitude of the electric field contributed by the Hall current contains a term linear in the field. That is, for one direction of magnetic field the x component of electric field, for example, is coupled to the y component through a positive coefficient, and for the other direction of magnetic field, it is coupled through a negative coefficient. Therefore, the total electric field in the plasma is changed when the dc magnetic field is reversed, or alternatively, when the direction of propagation is reversed for fixed magnetic field. Consequently, the reflection coefficient at the interface between free space and InSb is nonreciprocal.

An explanation for the nonreciprocal reflection based on the changes in electron orbits in a magnetoplasma was given by Pershan [7] and by Davies [8]. These arguments are extended here. Consider the situation when two identical waves are traveling through a plasma at equal but opposite angles to the vertical (see Fig. 1 without dielectric). In the absence of a dc magnetic field, the ratio of the x and y components of the electric field in a plasma is given by

$$\frac{E_y}{E_x} = \frac{-\sin\theta}{(K_\perp - \sin^2\theta)^{1/2}} \tag{19}$$

where

$$K = K_L - \frac{\omega_p^2}{\omega(\omega - j\nu)}\cdot \tag{20}$$

If the plasma is lossy, i.e., if $K_\perp$ is complex, the electric field in the plasma is elliptically polarized in the plane of incidence. Hence the orbits of electrons responding to this electric field are also elliptic. These elliptical motions can be decomposed into two oppositely rotating circular orbits with different radii. When a transverse dc magnetic field is applied, the radius of each circle is increased or decreased depending on the direction of the field. The resulting electron orbits obtained by summing the two oppositely rotating circular orbits may be drastically different from those without the field. That is, for one sense of magnetic field, the ellipse will be flatter than the case with no field, and for the other direction of field the ellipse will be more round, as shown in Fig. 6.

The explanation based on changes in electron orbits with reversal of the magnetic field (or equivalently, reversal of direction of propagation) also explains why electron collisions (or loss) must be present; if collisions do not take place, the reversal of the direction of propagation does not change the magnitude of the reflection coefficient but only its phase. Also if the collision rate is too high, only small nonreciprocal reflection takes place. The orbit of electrons in either a lossless or very lossy medium is almost linear. This linear polarization can be decomposed into right and left circular polarizations with equal radii. Application of a dc magnetic field causes one component to increase in magnitude and the other to decrease, and hence the polarization becomes elliptic. Reversing the field causes the whole process to reverse, but the orbits for the two directions of field are identical. Therefore, no nonreciprocal reflection is expected, but there is a change in phase, as can be seen from (18).

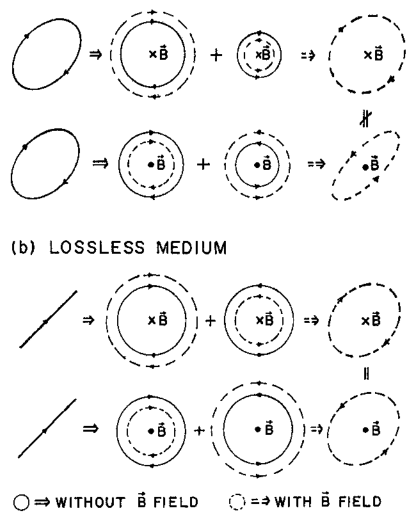

Fig. 6. Pictorial explanation for nonreciprocal reflection.

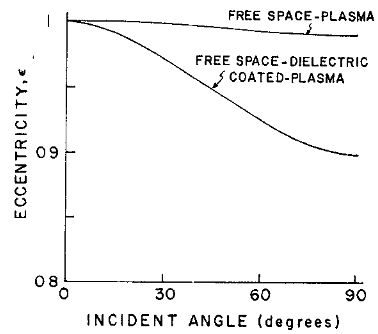

Fig. 7. Eccentricity ϵ of electron orbits in InSb as a function of incident angle. Geometry considered is shown in Fig. 1, with $\theta = 50°$, $B = 0$, and $l = 250\ \mu m$.

From the discussion given above, it appears that a maximum difference in reflection from a magnetoplasma with reversal of the dc magnetic field would take place if the orbit of electrons with $B = 0$ is nearly circular. The orbit cannot be completely circular, as can be shown from (19). Thus let us investigate the eccentricity ϵ of the orbit of electrons. With $B = 0$, ϵ as a function of incident angle θ is shown in Fig. 7 for two boundary conditions. As the incident angle increases, the eccentricity decreases, i.e., an electron orbit becomes more circular, thus we expect that the difference in reflection from a magnetoplasma with reversal of the dc magnetic field should increase with incident angle. However, at very large incident angles (over 85°) the reflection is quite large and hence only a small EM wave is transmitted into the plasma. Thus the change in reflection with reversal of the dc magnetic field decreases at very large incident angles simply because the wave

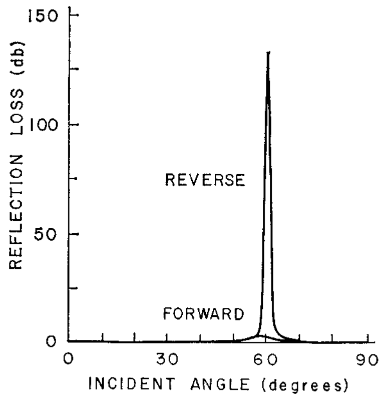

Fig. 8. Theoretical reflection loss of InSb at 337 μm as a function of incident angle. Geometry of isolator is shown in Fig. 1, with $B=16$ kG, $K_M=0.697$, and $l=276$ μm.

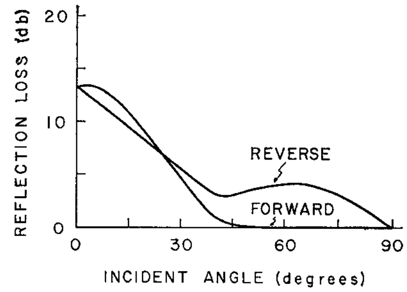

Fig. 9. Theoretical reflection loss for InSb at 118 μm as function of incident angle. The semiconductor is assumed to be in a magnetic field of 13.2 kG and in a medium with $K_M=50$.

does not interact much with the plasma. The eccentricities of the orbits for the case of a dielectric–plasma interface are much smaller than for the free space–plasma interface, as shown in Fig. 7; that is, the orbits of the electrons are much less linear, and hence greatly enhanced, nonreciprocal reflection can be observed for the case of a dielectric–plasma interface. Therefore, the combined effects of collisions, which are required to have an elliptic motion of electrons in a plasma without a magnetic field, and a dc magnetic field produce nonreciprocal effects.

B. Possible Refinements for Isolators

Large discrepancies between theoretical and experimental results are found at incident angles over 80° due to experimental difficulties as discussed in Section V. We investigate in this part means to shift the peak of the isolation curve to a lower incident angle.

A thin dielectric layer with a dielectric constant less than unity or even with a negative dielectric constant might be used to move the isolation peak to a more practical incident angle. Such a layer might be realized with either a semiconductor plasma or an artificial dielectric [9]. For example, when the dielectric layer on top of intrinsic InSb at room temperature has a dielectric constant of 0.697, it is possible to create the condition that no reflection takes place at a reasonable incident angle ($\theta=60°$) as shown in Fig. 8. However, the peak of the isolation curve is very critical with the incident angle, and hence with carrier density, mobility, and dc magnetic field. This sharpness of the isolation curve is due to the critical impedance match which results from the large impedance difference between free space and the InSb. However, the sharpness of the isolation curve could be made broader by the use of multiple layer matching transformers [10]. It may be possible to make use of this sharpness of isolation for the development of angle resolving devices. This sharpness which exists at 337 μm with InSb does not exist at 118 μm. The theoretical result for intrinsic InSb at 284 K and wavelength of 118 μm shows a very broad reflection-loss curve as a function of incident angle and an excellent ratio of isolation to forward insertion loss of about 50 in the decibel scale as shown in Fig. 9. The reverse loss can be increased by multiple reflection. This result indicates that the development of a practical and very efficient reflection-beam isolator should be possible using solid-state magnetoplasmas.

References

[1] N. F. Barber and D. D. Crombie, "V. L. F. reflections from the ionosphere in the presence of a transverse magnetic field," *J. Atmos. Terr. Phys.*, vol. 16, pp. 37–45, Oct. 1959.
[2] J. M. Seaman, "Nonreciprocal reflection of microwaves from a solid state magnetoplasma," M.S. thesis, Univ. Colorado, Boulder, Aug. 1969.
[3] R. E. Hayes and W. G. May, "The use of semiconductors in nonreciprocal devices for submillimeter wavelengths," in *Proc. Symp. Submillimeter Waves.* New York: Polytechnic Press, 1970, pp. 237–250.
[4] M. Kanda, "Study and applications of nonreciprocal behavior in solid state magnetoplasmas at millimeter and submillimeter wavelength," Ph.D. dissertation, Univ. Colorado, Boulder, Aug. 1971.
[5] M. Kanda and W. G. May, to be published.
[6] K. H. Breeden and A. P. Sheppard, "A note on the millimeter and submillimeter wave dielectric constant and loss tangent value of some common materials," *Radio Sci.*, vol. 3, pp. 205, Feb. 1968.
[7] P. S. Pershan, "Magnetooptical effects," *J. Appl. Phys.*, vol. 38, pp. 1482–1490, 1967.
[8] K. Davies, *Ionospheric Waves.* Waltham, Mass.: Blaisdell, 1969.
[9] A. F. Harvey, *Coherent Light.* New York: Wiley, 1970.
[10] L. Young, "Synthesis of multiple antireflection films over a prescribed frequency band," *J. Opt. Soc. Amer.*, vol. 51, pp. 967–974, Sept. 1961.